

Transient response of slot coating flow to periodic fluctuation in coating gap

Eduardo de Britto Perez, ebperez@mmm.com

Marcio da Silveira Carvalho, msc@puc-rio.br

Department of Mechanical Engineering, PUC – Rio, Rua Marquês de São Vicente, 225, Rio de Janeiro, RJ 22453-900

Abstract. Slot coating is a standard coating method for high precision coatings. Several authors have studied its coating window for steady state operation, but in manufacturing operations time dependent events are always present and specific transient analysis are very helpful. In this paper a transient analysis of slot coating process is performed to show the coating thickness variation response to an ongoing oscillation of the coating gap. Different die lip geometries and process parameters are tested and the respective impact on coating thickness is assessed by computer aided simulation. Results show that amplitude of the coating thickness variation on a given gap oscillation amplitude depends strongly on oscillation frequency, downstream and upstream lip geometries and capillary number. Also the results indicate the presence of a local optimum (minimum amplitude of thickness variation) for low frequencies in the space variables of coating gap against vacuum level.

Keywords: slot coating, transient analysis, frequency response.

1. INTRODUCTION

Products requiring high precision continuous coatings, such as optical films, are common in the coating industry. In most cases, final coating thickness variation higher than 2% is not acceptable. Slot coating is one of the preferred methods when high precision is required and several studies focusing on its steady state analysis (Higgings and Scriven, 1980) (Sartor, 1990) were made to determine the operating window of the process. However, full understanding of coating flows requires not only the two-dimensional, steady state solution of the governing equations, but also the sensitivity of those flows to small upsets.

An effort to understand the impact of the coating gap periodic oscillation on down web thickness variation is made using computer aided simulation (Gates, 1999) (Romero and Carvalho, 2008). Different slot die lip geometries and process conditions are tested and the respective amplification factors, Eq. (3), as a function of gap oscillation frequencies are reported. Among all process variables that may impact on coating thickness, the coating gap adjust and the vacuum level are particularly important because are easily changed by the process engineer. Two dimensional contour plots of the amplification factor in the space of coating gap against vacuum level are reported for some geometries, and interesting results shows up about their optimal conditions. The liquid is assumed Newtonian and computations are made at low capillary (up to 1.6) and Reynolds numbers.

The transient free surface flow with appropriate boundary conditions is solved by the Galerkin / finite element methods, with time integration by a predictor-corrector algorithm. The set of non-linear algebraic equations for the finite element basis functions coefficients at each time step is solved by Newton's method.

2. PROBLEM DESCRIPTION

Periodical coating gap (see Fig. 2) oscillation can be caused by back up roll run out or external sources of vibration not properly dampened by the die mounting structure. Coating gap oscillation, Eq. (1), is modeled as a sine function where H_0 (0.100 mm) is the coating gap at steady state and H_m (0.010 mm) is the oscillation amplitude.

$$H(t) = H_0 + H_m \sin(\omega t) \quad (1)$$

$$h(t) = h_0 + h_m \sin(\omega t + \phi) \quad (2)$$

$$\alpha(\omega) = \frac{h_m(\omega)}{H_m} \quad (3)$$

The final response of the flow to the gap oscillation is a down web coating thickness variation, Eq. (2), at which the amplitude (h_m) depends on the gap oscillation frequency (ω). As shown by Romero and Carvalho (2007), the frequency of the thickness variation is the same of the coating gap oscillation, although a phase lag (ϕ) may exist. Coating thickness at steady state (h_0) is set to 0.050 mm.

At each frequency the amplification factor, Eq. (3), which gives the ratio between the amplitude of the down web coating thickness variation to the amplitude of coating gap oscillation, can be calculated from the transient response of the flow.

The goal is to find die lip designs and process conditions that reduce the amplification factor over the entire frequency range, or at least, in a small range of interest.

3. MATHEMATICAL MODEL

The mathematical model to describe the flow in the coating bead is shown in Fig. 1.

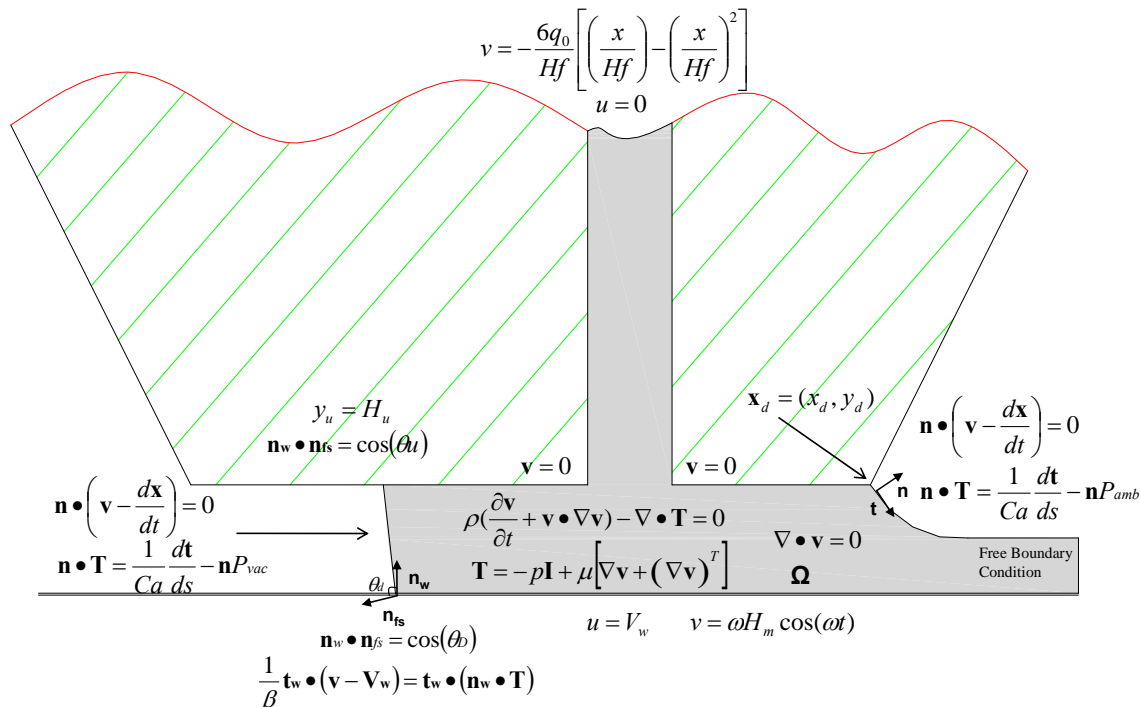


Figure 1. Mathematical model of the slot coating flow

The flow domain is governed by the two dimensional Navier-Stokes equation and a set of proper boundary conditions.

- (1) At air-liquid interfaces, capillary and pressure forces take place with the additional condition that there is no flow across this interface (kinematic boundary condition);
- (2) At liquid-solid interfaces, the no-slip and no-penetration boundary conditions are set;
- (3) At liquid inlet, a full developed velocity profile is prescribed;
- (4) At liquid outlet, it is assumed the “free boundary condition”, and the force is given by

$$\mathbf{n} \cdot \mathbf{T} = -p\mathbf{n} + \mathbf{n} \cdot \left[\nabla \mathbf{v} + (\nabla \mathbf{v})^t \right] \quad (4)$$

- (5) At the dynamic contact line, the Navier slip boundary condition is imposed and a contact angle is prescribed;
- (6) Finally, the downstream contact line is pinned at the downstream lip corner.

The local velocity derivative $\frac{\partial \mathbf{v}}{\partial t}$ must be adjusted to take into account the mesh variation (“node velocity”) as discussed by (Christodoulou, 1992):

$$\frac{\partial \mathbf{v}}{\partial t} = \overset{0}{\mathbf{v}} - \overset{0}{\mathbf{x}} \cdot \nabla \mathbf{v} \quad (5)$$

Where: $\overset{0}{\mathbf{v}}$ = local rate of velocity variation in nodal point;
 $\overset{0}{\mathbf{x}}$ = mesh velocity.

Substitution of Eq. (5) in the momentum equation leads to:

$$\rho \left[\mathbf{v} + (\mathbf{v} \cdot \mathbf{x}) \bullet \nabla \mathbf{v} \right] = \nabla \bullet \mathbf{T} \quad (6)$$

The initial condition is necessary to solve the transient problem and this is given by the steady state solution of the flow.

$$\mathbf{v}(t=0) = \mathbf{v}_0(x,y) \quad p(t=0) = p_0(x,y) \quad (7)$$

The momentum, continuity and constitutive equations with all boundary conditions on Fig. 1 form a system of non linear partial differential equations defined in a domain Ω , which is unknown due the presence of free surfaces and the imposed oscillation.

In order to solve the system of equations mentioned above, it is necessary to rewrite them in a fixed known domain, Ω_d , with an additional cost of including the equations that map the domains. These equations are bijective applications, $\mathbf{x}(\xi)$, between each point of the domains. Where \mathbf{x} is the position vector of one point of the real domain and ξ is the position vector of one point in the reference domain.

Rectangular reference domains are frequently used by their simple representation. If the real domain is complex, it can be partitioned and mapped to several rectangular shaped reference domains

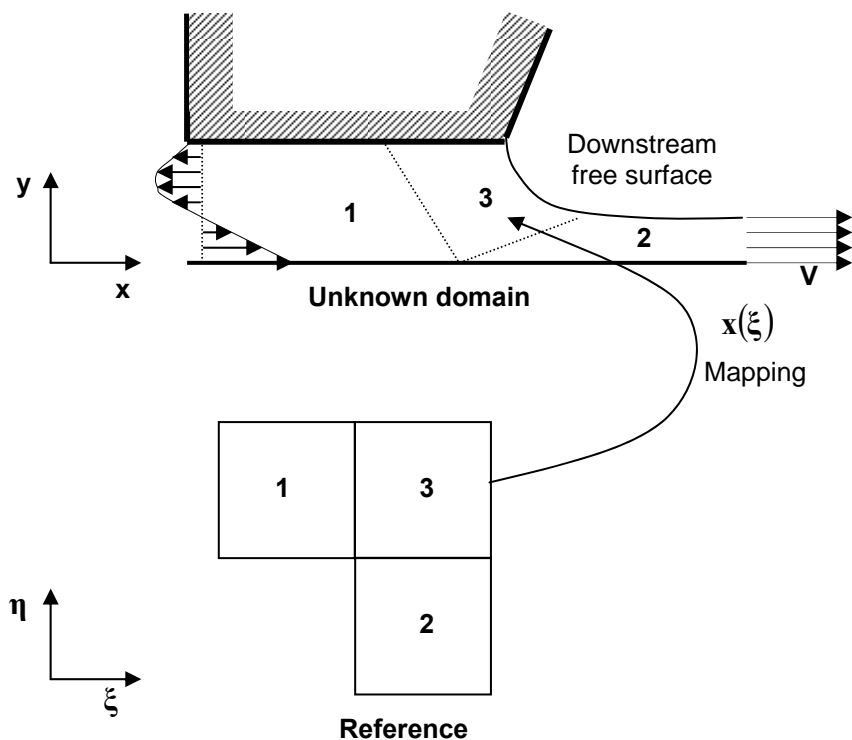


Figure 2 – Mapping between the real and reference domains (Romero and Carvalho, 2005)

There are some techniques to define the mapping equations and all them must obey 2 rules:

- (1) Boundary points of the real domain must map boundary points of the reference domain;
- (2) Mapping must be invertible.

Item (2) means that the determinant of the Jacobian matrix of the mapping equation must be different to zero.

$$\det(\mathbf{J}) \neq 0 \quad (8)$$

In two dimensions the Jacobian matrix (transpose) is given by:

$$\nabla_{\xi} \mathbf{x} \equiv \mathbf{J} = \begin{pmatrix} \frac{\partial x}{\partial \xi} & \frac{\partial y}{\partial \xi} \\ \frac{\partial x}{\partial \eta} & \frac{\partial y}{\partial \eta} \end{pmatrix} \quad (9)$$

Partial derivatives of any quantity in the real domain can be represented by partial derivatives in the reference domain Ω_0 using Eq. (10).

$$\begin{pmatrix} \frac{\partial \phi}{\partial x} \\ \frac{\partial \phi}{\partial y} \end{pmatrix} = \mathbf{J}^{-1} \begin{pmatrix} \frac{\partial \phi}{\partial \xi} \\ \frac{\partial \phi}{\partial \eta} \end{pmatrix} \quad (10)$$

$$\mathbf{J}^{-1} = \frac{1}{\det(\mathbf{J})} \begin{pmatrix} \frac{\partial y}{\partial \eta} & -\frac{\partial y}{\partial \xi} \\ -\frac{\partial x}{\partial \eta} & \frac{\partial x}{\partial \xi} \end{pmatrix} \quad (11)$$

$$d\Omega = \det(\mathbf{J})d\Omega_0 \quad (12)$$

Elliptical equations to generate meshes have been shown useful to create smooth meshes.

$$\nabla \cdot [D_\xi \nabla \xi] = 0, \quad \nabla \cdot [D_\eta \nabla \eta] = 0 \quad (13)$$

D_ξ and D_η are coefficients that control the mesh spacing in the domain, and as the mesh generation equations are written in the real domain, $\xi(\mathbf{x})$, they also need to be rewrite in the reference domain, $\mathbf{x}(\xi)$.

Equations (13) must be included in the system of differential equations of section 3 and their solution to each time step determines the position of the mesh nodes.

Proper boundary conditions for mesh equations must be defined and depends if the boundary is fixed or a free surface.

The weighted residual method coupled with Garlekin base functions of finite elements was used to solve the partial differential non linear equations. Time integration was performed using a predictor-corrector algorithm.

4. COMPUTER AIDED ANALYSIS

A two-dimensional view of slot coating bead is depicted in Fig. 2.

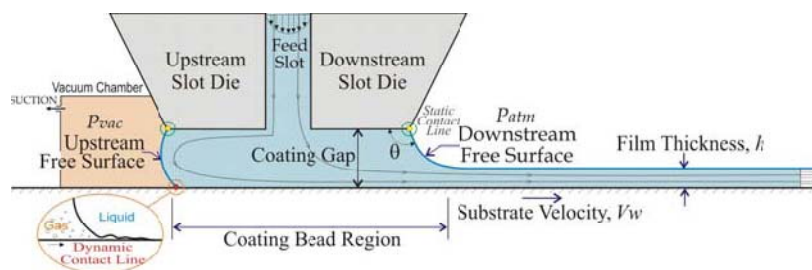


Figure 2. Two-dimensional view of slot coating die (Romero, ISCST 2006)

Four different die designs, Fig. 3, were considered to analyze the effect of geometry on the frequency response of the flow in terms of the amplification factor, as shown in Fig. 4 and 5. The geometric variables were the upstream coating gap (H_u), downstream coating gap (H_d), downstream lip length (L_d) and convergence angle of downstream lip (β_d). Downstream static contact line is assumed pinned at downstream corner of the die lip, while upstream static contact line is free to move under the upstream die lip, with a prescribed angle. H_f is the slot width, kept constant for all cases.

Table 1. Die lip geometries for the computer aided simulations of Fig. 4 and Fig. 5.

Die Code	H_u (mm)	H_d (mm)	L_d (mm)	H_f (mm)	β_d (mm)	L_u (mm)
Slott1	0.100	0.100	0.600	0.100	90°	0.600

Slott2	0.150	0.100	0.600	0.100	90°	0.600
Slott1D1	0.100	0.100	0.300	0.100	90°	0.600
Slott1DC	0.100	0.100	0.600	0.100	92°	0.600

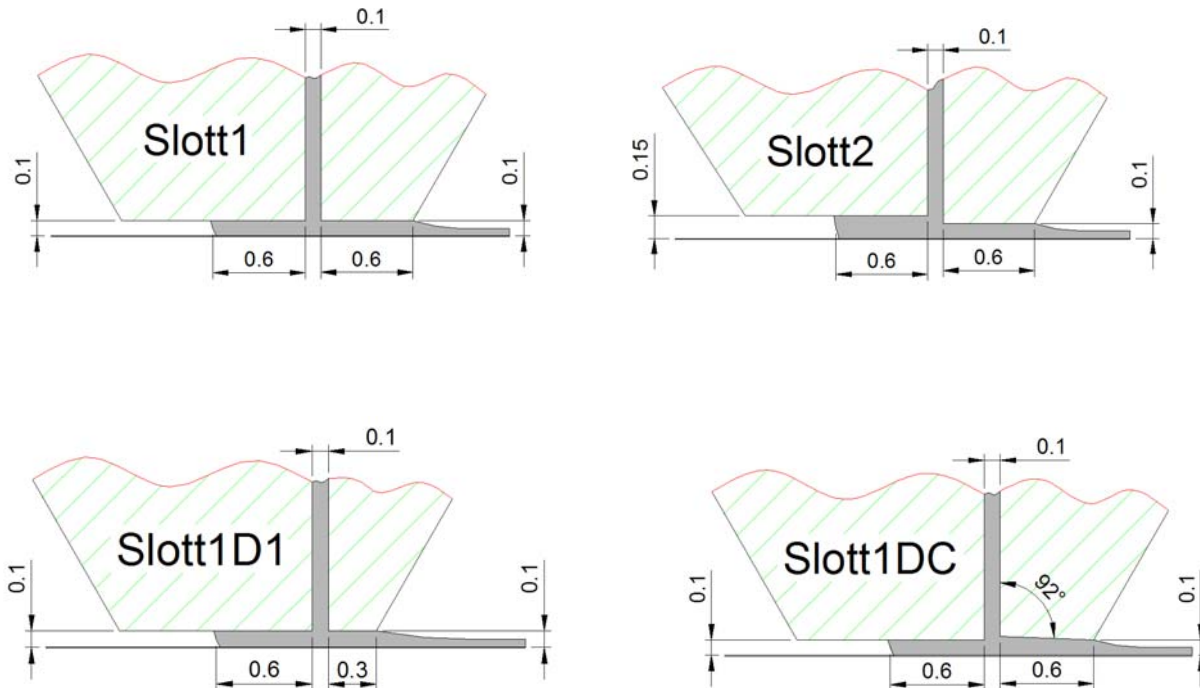


Figure 3. Die lip designs

Process parameters for the analysis presented in Fig. 4 and Fig. 5 are shown on Tab. 2.

Table 2. Process parameters for the computer aided simulations if Fig. 4 and Fig. 5.

$Ca = \frac{\mu V}{\sigma}$	X_{dcl} (mm)	$Re = \frac{\rho V H_d}{\mu}$	$Vac = \frac{Pvac H_d}{\sigma}$	$Pvac$ (Pa)	V_w (m/s)	μ (mPa.s)	ρ (Kg/l)	σ (dyn/cm)
0.05	0.6	0.33	2.33	-1380	0.1	30	1	60
0.2	0.6	0.33	8.67	-1300	0.1	30	1	15

Where: X_{dcl} is the position of the dynamic contact line;
 $Pvac$ is the upstream vacuum;
 μ is the dynamic viscosity;
 ρ is density;
 σ is the liquid surface tension.

5. RESULTS AND DISCUSSION

Figures 4 and 5 present the influence of the downstream die lip design and upstream gap on the amplification factor. The responses have the same general behavior. The amplification factor approaches zero as the frequency approaches zero, i.e. as the flow becomes quasi-steady. At high frequency, the amplification factor approaches one, the oscillation is so fast that the downstream free surface does not have time to respond, staying on the same position, leading to amplitude equal to the gap disturbance amplitude.

For all cases there is a maximum on the amplification factor at an intermediate frequency range.

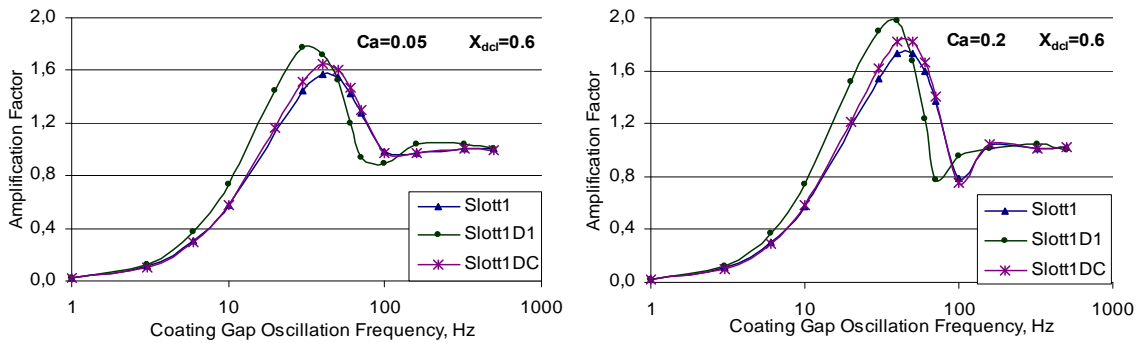


Figure 4. Influence of downstream lip geometry on amplification factor

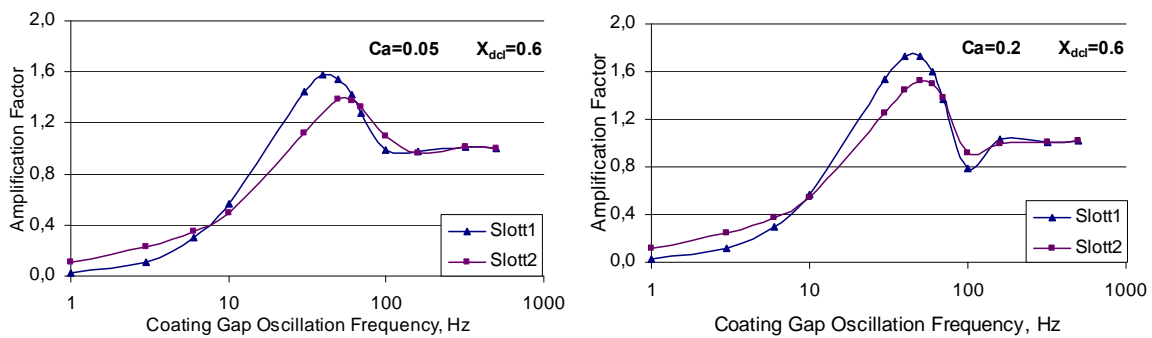


Figure 5. Influence of upstream gap on amplification factor

The results suggest that the downstream die lip shapes that promote higher pressure drop lead to smaller amplification factors in the region of the peak frequency.

At low frequencies, the smaller upstream gap showed better results, while at intermediate frequencies the opposite is true. As frequencies tends to zero, there is a quasi-static regime where the liquid bead responds promptly to gap oscillation and reduces coating thickness variation amplitude.

Coating gap and vacuum level are basic process parameters in a slot coating process and are the first options to reduce coating thickness variation amplitude when an ongoing coating oscillation is present.

Figure 6 and 7 shows contour plots of the amplification factor at a low and a next to peak frequency for *slott1* and *slott2* geometries. Process parameters are listed in tab. 3.

Table 3. Process parameters for contour plots.

$Ca = \frac{\mu V}{\sigma}$	h_0 (m)	V_w (m/s)	μ (mPa.s)	ρ (Kg/l)	σ (dyn/cm)
0,2	$0,050 \times 10^{-3}$	0.1	30	1	15

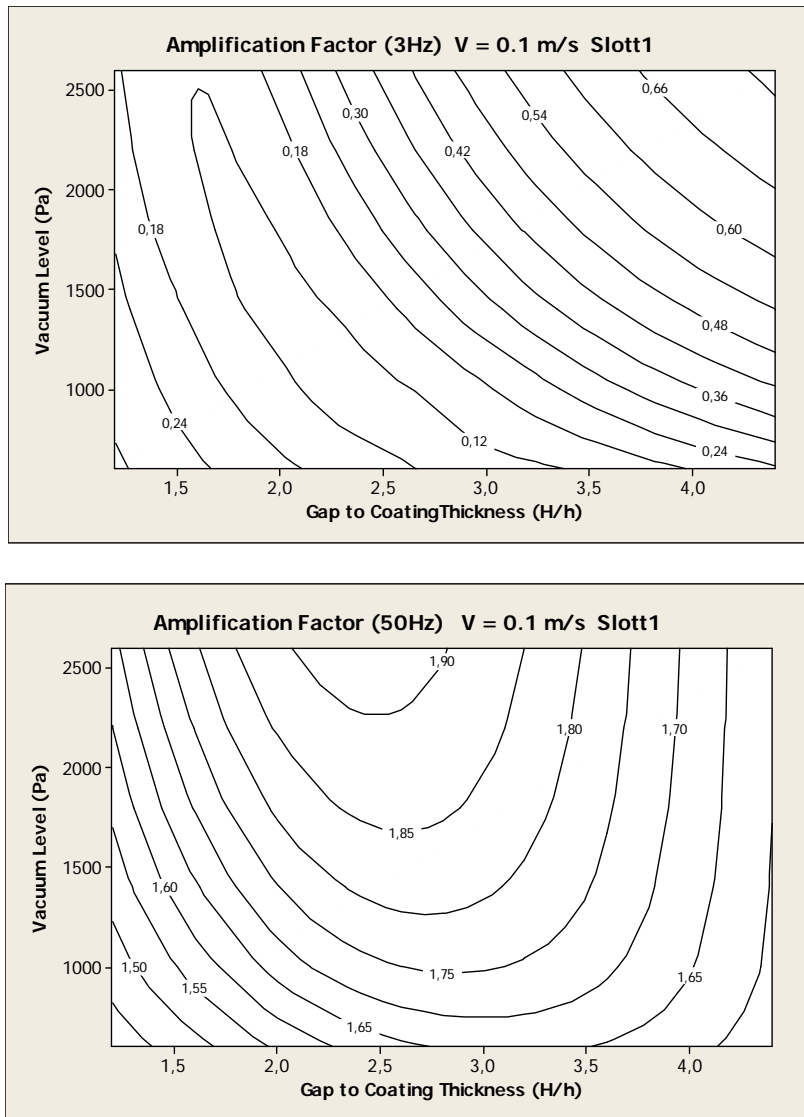


Figure 6. Contour plot of coating gap against vacuum level for *slott1* and process parameters in Tab. 3.

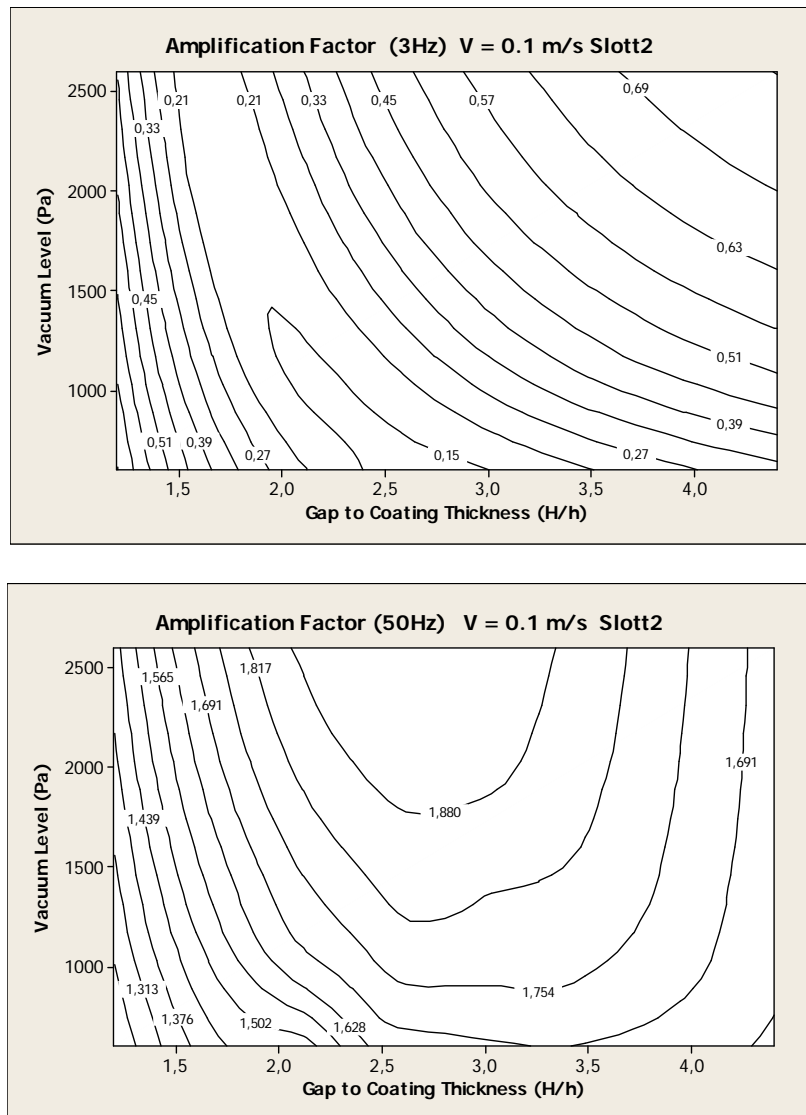


Figure 7. Contour plot of coating gap against vacuum level for *slott2* and process parameters in Tab. 3.

The contour plots for both geometries show a local optimum region (minimum amplification factor) for low frequency and the location of this region is about the same in the two plots.

At near to peak frequency the optimum region is located in the lower left corner of the contour plot for both geometries, i.e. the ideal operating condition is at low vacuum and small gap.

The fact that different geometries show similar optimum conditions suggests a simple rule to guide process engineers when trying to reduce coating thickness variation amplitude. The idea is to classify the gap oscillation frequency as low, intermediate (near to peak) and high frequencies.

Low frequencies and intermediate frequencies follow the optimum adjust mentioned above and for high frequencies there is no optimum condition, since the amplification factor is insensitive to variation on geometry or process parameters and close to one.

As this classification depends on actual line speed, Fig. 8 suggests that the location of the peak is approximately linear with line speed.

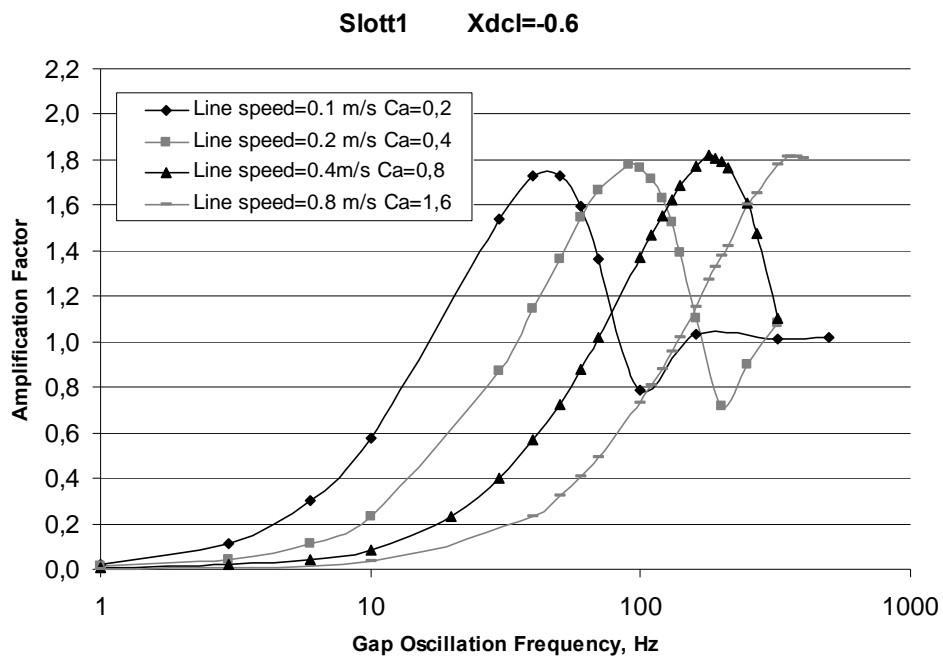


Figure 8. Frequency response of amplification factor as function of line speed

Based on this observation, the classification suggested is detailed in Tab. 5. Intermediate frequencies are located between low and high frequency values.

Table 3. Classification of gap oscillation frequencies based on line speed.

<i>Line speed (m/s)</i>	<i>Frequency range of peak (Hz)</i>	<i>Low frequencies (Hz)</i>	<i>High frequencies (Hz)</i>
0.1	40 - 50	0 - 20	> 200
0.2	80 - 100	0 - 40	> 400
0.4	160 - 200	0 - 80	> 800
0.8	320 - 400	0 - 160	> 1600

Application of this rule works for *slott1* at 0.2 m/s, as shown in Fig. 9

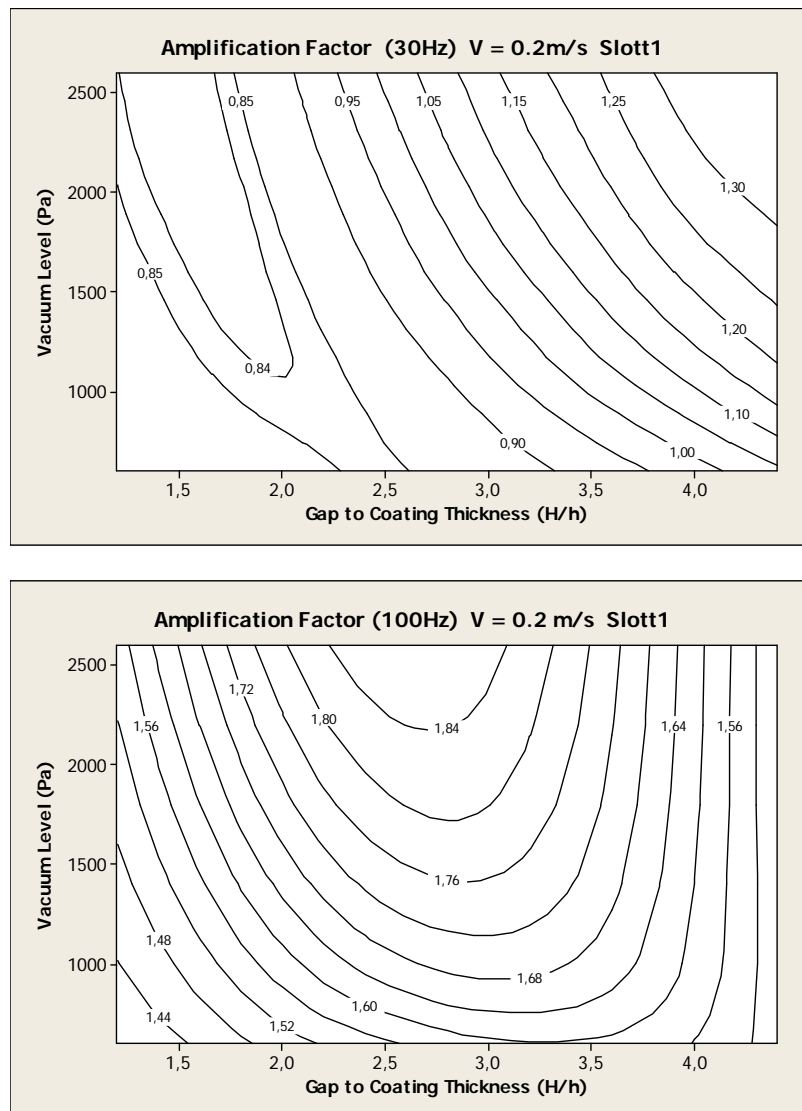


Figure 9. Contour plot of coating gap against vacuum level for *slott1* at 0.2 m/s other process parameters (except capillary number) in Tab. 3.

Geometry *slott1D1* also showed the same behavior on contour plots at low and intermediate frequencies, what reinforce the usefulness of the proposed classification and optimization strategy.

6. REFERENCES

- B. G. Higgins and L. E. Scriven, 1980, "Capillary pressure and viscous pressure drop set bounds on coating bead operability". Chemical Engineering Science, vol. 35, 673-682.
- I. A. Gates, 1999, "Slot coating flows: feasibility, quality". Ph.D. thesis, University of Minnesota.
- L. Sartor, 1990, "Slot coating: fluid mechanics and die design". Ph.D. thesis, University of Minnesota.
- O. J. Romero and M. S. Carvalho, 2008, "Response of slot coating flows to periodic disturbances". Chemical Engineering Science, vol. 63, 2161-2173.

7. RESPONSIBILITY NOTICE

The authors are the only responsible for the printed material included in this paper.